ORIGINAL PAPER

Suppression of Thiol-Dependent Antioxidant System and Stress Response in Methicillin-Resistant *Staphylococcus aureus* by Docosanol: Explication Through Proteome Investigation

Selvaraj Alagu Lakshmi[1] · Krishnan Ganesh Prasath[1,2] · Kannapiran Tamilmuhilan[1] · Adimoolam Srivathsan[1] · Raja Mohamed Beema Shafreen[1,3] · Thirupathi Kasthuri[1] · Shunmugiah Karutha Pandian[1]

Abstract

The present study was aimed to investigate the effect of docosanol on the protein expression profile of methicillin-resistant *Staphylococcus aureus* (MRSA). Thus, two-dimensional gel electrophoresis coupled with MALDI-TOF MS technique was utilized to identify the differentially regulated proteins in the presence of docosanol. A total of 947 protein spots were identified from the intracellular proteome of both control and docosanol treated samples among which 40 spots were differentially regulated with a fold change greater than 1.0. Prominently, the thiol-dependent antioxidant system and stress response proteins are downregulated in MRSA, which are critical for survival during oxidative stress. In particular, docosanol downregulated the expression of Tpx, AhpC, BshC, BrxA, and YceI with a fold change of 1.4 ($p = 0.02$), 1.4 ($p = 0.01$), 1.6 ($p = 0.002$), 4.9 ($p = 0.02$), and 1.4 ($p = 0.02$), respectively. In addition, docosanol reduced the expression of proteins involved in purine metabolic pathways, biofilm growth cycle, and virulence factor production. Altogether, these findings suggest that docosanol could efficiently target the antioxidant pathway by reducing the expression of bacillithiol and stress-associated proteins.

Keywords Methicillin-resistant *Staphylococcus aureus* · Docosanol · Two-dimensional electrophoresis · Proteome · Antioxidants · Oxidative stress

Introduction

Methicillin-resistant *Staphylococcus aureus* (MRSA), Gram-positive bacteria from the phylum *Firmicutes*, is a superbug, resistant to commonly deployed first-line β-lactam antibiotics [1]. Successful treatment is hampered due to bacterial biofilms and constant adaptation to new antibiotics. Biofilm-associated drug resistance plays a major role in the pathogenesis of acute and chronic infections in clinical settings. Medical devices such as oral implants, endotracheal tubes, prosthetic joints, contact lenses, urinary catheters, heart valves, and pacemakers are susceptible to bacterial colonization [2–6]. *Staphylococcus aureus* utilizes numerous strategies to defend itself from hostile environments such as disinfectants, antibiotics, oxidative stress, and host defence mechanism. One effective host-encoded strategy to kill *S. aureus* is the production of high levels of oxidants; however, *S. aureus* overwhelms the oxidative-killing mechanisms mounted by immune cells [7].

During aerobic cellular respiration, oxygen reacts with glucose for energy production and subsequently results in primary byproducts such as carbon dioxide and water. But when aerobic respiration is incomplete, it generates reactive oxygen species (ROS) such as superoxide (O_2^-), hydrogen peroxide (H_2O_2), and hypochlorous acid (HOCl) as normal cellular metabolites. ROS is also produced by myeloperoxidase that is released from the activated macrophages and neutrophils during bacterial infection [8, 9]. However, pathogenic bacteria are equipped with loads of immune-modulatory proteins to evade the host's innate defence. The ROS generated either from endogenous or exogenous sources

✉ Shunmugiah Karutha Pandian
pandiansk@gmail.com

1 Department of Biotechnology, Alagappa University, Science Campus, Karaikudi, Tamil Nadu 630003, India

2 Department of Biotechnology, Sri Venkateswara College of Engineering, Sriperumbudur, Tamil Nadu 602117, India

3 Department of Biotechnology, Dr. Umayal Ramanathan College for Women, Alagappapuram, Karaikudi, Tamil Nadu 630003, India

have the ability to oxidize biological macromolecules such as lipids, proteins, carbohydrates, fatty acids, and nucleotides, thereby resulting in ROS-induced cellular damage. In order to overcome the challenges induced by electrophilic ROS, the antioxidant system comes into play to protect the cell from damaging effects [10]. In particular, low molecular weight thiol systems such as glutathione (GSH) utilizing glutaredoxin (Grx) and thioredoxin (Trx) systems are the central players in bacterial protection. Despite this, Grx and Trx act as a backup system for each other. Studies with strains defective in either Grx or Trx system showed no significant effect on growth phenotype. However, mutant strain (lacking both Grx and Trx) was found to be lethal. Recently, analogs to GSH termed bacillithiol (Brx) and mycothiol were found in low G+C *Firmicutes* and high G+C Actinobacteria, respectively [11]. But the specific function of these low molecular thiols and their importance in bacterial systems, especially in human pathogens remains to be fully elucidated. The development of inhibitors against the antioxidant system of MRSA is very promising and could lead to new anti-MRSA drugs [12]. The antivirulence effect of docosanol such as the survival rate of MRSA in healthy human blood and the antioxidant property has been reported earlier [13]. However, the mechanism by which docosanol targets MRSA is not known. Thus, the present study was conducted to probe how docosanol treatment affects MRSA and the critical key players involved in the suppression of virulence factors.

Materials and Methods

Bacterial Strains and Growth Conditions

All the chemicals used in this study were purchased from Sigma Aldrich, USA, and GE Healthcare, USA unless otherwise noted. *S. aureus* ATCC 33591 used in this study was purchased from HiMedia Laboratories Pvt. Ltd. India. The strain was grown in tryptic soy broth (TSB) supplemented with 1% (w/v) sucrose [14] and incubated at 37 °C for 24 h with constant rotation at 160 rpm. MRSA was treated with 500 µg/mL of docosanol (Sigma Aldrich, USA) [13]. In the case of control, MRSA was treated with methanol.

Intracellular Protein Preparation

Control and treated cells (200 mL) were collected by centrifugation at 7000×*g*, at 4 °C for 20 min. For intracellular protein extraction, the cell pellet was washed twice with distilled water and resuspended in sample buffer (7 M urea, 2 M thiourea, 4% 3-[(3-cholamidopropyl)-dimethylammonio]-1-propanesulfonate (CHAPS), 40 mM Dithiothreitol (DTT)). The samples were sonicated in Vibra cell Ultrasonic Processor VCX-750, USA with an amplitude of 25%, 1000 J energy, and a pulse of 10 s on and 10 s off. The whole process was carried out on the ice. In Gram-positive bacteria, the intracellular protease complex contributes to cell survival in a stress environment [15] and moreover, they cleave the peptide bond in active proteins. In order to prevent the activity of proteases, the cell lysates were sonicated in the presence of a bacterial protease cocktail (P8465, Sigma-Aldrich USA), 5 mM Phenyl ethyl sulphonyl fluoride (PMSF), and 1 mM Ethylene diamine tetraacetic acid (EDTA). Cell debris was removed by centrifugation at 11,000×*g* for 30 min at 4 °C and the supernatants containing intracellular proteins were subjected to phenol extraction. An equal volume of tris-saturated phenol was added to the protein sample and incubated at 70 °C for 10 min followed by incubation at 4 °C for 15 min. The proteins in the organic phase were collected by centrifugation at 10,000×*g* for 15 min at 4 °C and precipitated with 3 volumes of ice-cold acetone. The tubes were incubated at −20 °C for 10 min and the precipitated proteins were recovered through centrifugation. Samples were air-dried and dissolved in sample buffer [16]. The protein concentration was quantified through Bradford's method using BSA as the standard [17].

Two-Dimensional gel Electrophoresis (2DGE)

A protein concentration of 500 µg was mixed with rehydration buffer containing 7 M urea, 2 M thiourea, 2% CHAPS, 0.28% DTT, 0.002% Bromophenol blue, 0.5% IPG buffer (pH 4–7; GE Healthcare, USA) and 1.2% destreak reagent. For separation of proteins in first-dimension, samples were applied to the slots of Immobiline DryStrip Reswelling Tray and overlaid with the Immobiline DryStrips gel (IPG strips) (pH 4–7 non-linear, 18 cm) (GE Healthcare, USA, Cat. No. 17123301). Passive in-gel rehydration was performed at 20 °C for 18 h. The IPG strip was transferred to the IPG strip holder and covered with PlusOne DryStrip Cover Fluid (Amersham Biosciences, UK, Cat. No. 17-1335-01) to prevent drying. Isoelectric focusing (IEF) was performed in Ettan IPGphor 3 isoelectric focusing unit (GE Healthcare, USA) according to the manufacturer's instructions. After IEF, the IPG strips were subjected to equilibration with equilibration buffer I containing 6 M urea, 30% glycerol (w/v), 2% SDS (w/v), and 1% DTT (w/v) in 50 mM Tris–HCl buffer (pH 8.8) for 15 min and a second equilibration with equilibration buffer II containing 6 M urea, 30% glycerol (w/v), 2% SDS (w/v), and 2.5% iodoacetamide (IAA) (w/v) in 50 mM Tris–HCl buffer (pH 8.8) for 15 min.

For second-dimension separation of proteins, the IPG strips were placed on 22 cm × 22 cm × 1 mm 12.5% SDS-PAGE gel and overlaid with 0.5% agarose. Electrophoresis was performed in Ettan DALT six apparatus (GE Healthcare, USA) with an initial constant voltage of 10 mA/gel

for 1 h followed by 25 mA/gel until the tracking dye reaches the bottom of the gel. After electrophoresis, gels were incubated overnight in fixative solution (40% methanol (v/v), 10% glacial acetic acid (v/v), and 50% distilled H_2O) followed by washing thrice with distilled water (each 20 min). The gels were then stained using Coomassie Brilliant Blue G-250 staining solution [10% orthophosphoric acid (v/v), 10% ammonium sulphate (w/v), 20% methanol (v/v) and 0.12% Coomassie Brilliant Blue (CBB, w/v)] for 12 h in gel rocker [16, 18].

Image Analysis, In-Gel Digestion, and Peptide Extraction

The gels were destained with distilled water prior to scanning in Image Scanner III (GE Healthcare, USA) to remove the excess dye from the gel-matrix background. Images were documented and analysed using LabScan 6.0 software and Image Master 2D Platinum 7 (GE Healthcare, USA), respectively. The differentially expressed protein spots with fold change > 1.0 were excised from the gel and completely destained with 50% acetonitrile containing 25 mM ammonium bicarbonate (NH_4HCO_3). The gel pieces were then dehydrated using 100% acetonitrile for 10 min, vacuum dried, and digested with 400 ng of trypsin (prepared in 10 mM NH_4HCO_3, 10% acetonitrile; Sigma-Aldrich, USA) at 4 °C for 45 min. Samples were then overlaid with 50 µL overlay solution (40 mM NH_4HCO_3, 10% acetonitrile) and incubated at 37 °C for 16 h. Peptides were extracted using 50 µL extraction buffer containing 60% acetonitrile/0.1% Trifluoroacetic acid (TFA) by sonication, followed by subsequent extractions with 70% acetonitrile/0.1% TFA, 80% acetonitrile/0.1% TFA, and 100% acetonitrile. The fractions collected were pooled, vacuum dried, and resuspended in 5 µL resuspension buffer (0.1% TFA in 5% acetonitrile) [16].

MALDI-TOF/TOF/MS Analysis

The MALDI-TOF/TOF (AXIMA Performance, SHIMADZU, Japan) was calibrated with TOF- Mix™ (LaserBio Labs, France) in positive reflector mode. The TOF- Mix™ consists of seven different peptides such as Bradykinin 1–7 (757.3992), Angiotensin II (1046. 5418), Angiotensin I (1296. 6848), Glu1-Fibrinopeptide B (1570.6768), *N*-acetyl renin substrate (1800.943), Adrenocorticotropic Hormone (ACTH) fragment (1–17) (2093.0862), ACTH fragment (18–39) (2465.1983) and ACTH fragment (7–38) (3657.8576). Then, the peptides were sandwiched in 0.5 µL of α -cyano-4-hydroxy cinnamic acid matrix (Sigma-Aldrich, USA, 10 mg/mL) on the sample plate. The spectra of peptides were acquired in the form of monoisotopic pattern and evaluated by Shimadzu launchpad-MALDI MS software [19] and the peak harvesting was performed using the same software.

Bioinformatic Analysis and Functional Insights into Uncharacterized Proteins of MRSA

MS-FIT

The peptide mass fingerprinting (PMF) for the corresponding protein was evaluated using the MS-FIT proteomic tool (http://prospector.ucsf.edu/prospector/cgi-bin/msform.cgi?form=msfitstandard). The query sequences were analysed in MS-FIT by setting a minimum number of matched peptide masses as 4 [20]. The maximum mass tolerance was 50 ppm after an internal calibration using Mix™ (LaserBio Labs, France) and two missed cleavages for tryptic peptides were allowed. The modifications accepted were carbamidomethyl cysteines as constant with oxidation of methionine and acrylamide modified cysteines as the variable.

STRING and Gene Ontology (GO) Analysis

Differentially regulated proteins were analysed through the STRING database (https://string-db.org/cgi/input.pl?sessionId=QjOYe9SUqXhy&input_page_active_form=multiple_identifiers) for protein–protein interaction network [21]. In STRING analysis, the functional and physical protein associations were indicated in a full-network string with a confidence score of 0.700 (high). The active interactions sources comprise the experiments, databases, co-expression, neighborhood, gene fusion, and co-occurrence. The maximum number of interactors were no more than 10 in both the first and second shell. MCL clustering is used and the network is clustered to an inflation parameter of 3. Gene ontology (GO) analysis was performed to identify the key genes involved in biological processes, molecular function, and cellular components. Functional characterization of uncharacterized proteins that are differentially regulated in docosanol treatment in MRSA, was carried out according to the protocol described by Lakshmi et al. [22].

Statistical Analysis

All the experiments were performed in biological replicates with experimental triplicates for the proteomic analysis in both MRSA control and treated samples ($n = 3$). The differentially regulated protein spots were analysed by Image master 2D-platinum software. The differentially regulated spots were selected based on the statistical analysis by one-way ANOVA with $p < 0.05$. For MALDI-TOF/TOF, the extracted proteins were processed in experimental replicates ($n = 5$) and the peptide mass fingerprinting (PMF) for each corresponding protein sample was evaluated.

Results and Discussion

Intracellular Proteome Analysis of MRSA Treated with Docosanol

Proteins were resolved in 2DGE using a narrow range immobilized pH gradient (IPG) strip (pI 4–7) and the gels were scanned and documented using Image master 2D platinum software for identification of differentially expressed proteins. Zhang et al. [23] reported that IPG strip with a narrow pH range (4–7) resulted in better resolution, separation of combined protein spots, and detection of low abundance proteins. Similarly, *S. aureus* proteins separated on the pI range of 4–7 displayed well separation and distribution of protein spot throughout the region of pI 4–7 and allowed for safe, accurate excision and image identification [24, 25]. Besides, *S. aureus* proteins associated with virulence factor production, antimicrobial resistance, and oxidation–reduction process are spotted in the pI region of 4–7 [24]. Therefore, the IPG strip with a pI range of 4–7 was used in this current study for better resolution. A total of 947 spots were identified in the intracellular proteome of both control and docosanol-treated samples. From these, differentially expressed spots with fold change ≥ 1.0 were picked: based on the statistical analysis from one-way ANOVA, considering all the triplicate gels with *p* value < 0.05. Among 40 distinguished spots from intracellular proteins, two spots were found to be upregulated and 38 spots were found to be downregulated (Fig. 1). The list of differentially regulated proteins following exposure to docosanol in MRSA is given in Table 1. Functional protein–protein interaction network predicted through STRING database is given in Fig. 2. The interacting partners of RpsB are RplK, RpsF, RpsG, RpsL, RpsR, RpmB, RplL and hpf. Functional partners of PurQ are PurK, PurM, PurN, and PurL; and AhpC is Tpx. The edge intensity in Fig. 2 represents the high confidence score of the predicted functional associations. Through MCL clustering, proteins involved in major biological functions were clustered into cell adhesion (SspB, FnbA), detoxification and anti-oxidation (AhpC, Tpx), ribosome and translation regulator activity (AtpC, RimM, RpsB), purine biosynthesis (Apt, PurQ), TCA cycle (AzoR, SucC), and isoprenoid metabolism (Cmk and Fni). Among these cell adhesion, detoxification and anti-oxidation, purine biosynthesis, and TCA cycle are linked to biofilm development [26–29]. Differentially regulated proteins were grouped into three GO categories, biological process; molecular function; and cellular component (Fig. 3). In the biological process, the majority of the differentially regulated proteins were involved in metabolic (including catabolic, cellular, cellular nitrogen, organic substance, nitrogen compound, organonitrogen compound, phosphate-containing compound) and biosynthetic processes (organonitrogen compound, organic substance, cellular, aromatic compound, organophosphate, organic, and heterocycle compound). In molecular function, the majority of the differentially regulated proteins were involved in binding, organic or heterocyclic compound binding, and catalytic activity. At the cellular level, the differentially regulated proteins were primarily associated with intracellular and cytoplasm. Protein list in all three categories includes AhpC, Apt, ArgS, ArsC, AtpC, AtpD, AzoR, CrtN, Fni, FolE2, GpmA, MraZ, NadD, PgcA, PtpA, PtpB, PurL, PurQ, RecR, RimM, RplB, RpsB, RpsE, RpsG, RpsH, RpsK, RpsS, RsbW, SrrA, SspB, SucC, UreB, And UreC.
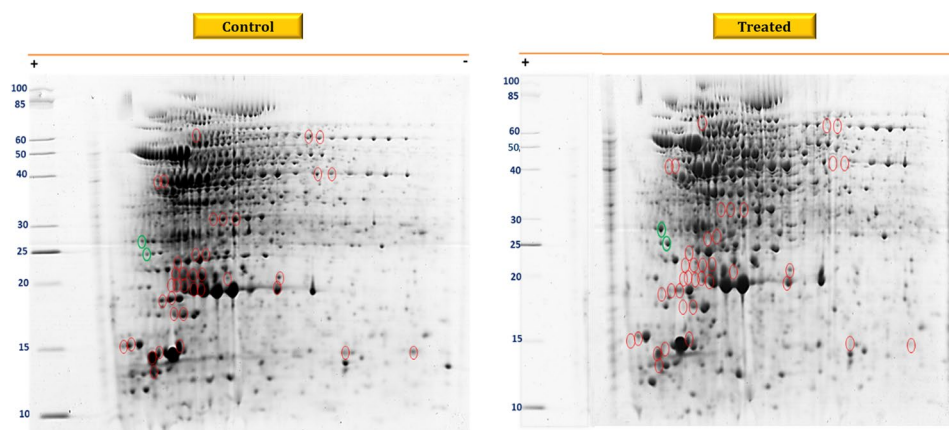
Fig. 1 Two-dimensional gel electrophoresis showing intracellular proteome from control and docosanol treated samples of MRSA. Proteins were analysed in the pH range of 4 to 7 (non-linear; 18 cm strip). Proteins were separated according to isoelectric point in the first-dimension and then by size in the second-dimension. Protein spots ($n=947$) identified from the intracellular proteome of both control and docosanol treated samples. Differentially expressed protein spots with fold change ≥ 1.0 are marked in green (upregulated; $n=2$) and red (downregulated; $n=38$) circles

Table 1 List of differentially regulated proteins in MRSA upon treatment with docosanol

S. no.	MW (Da)/pI	Protein name	UniProt ID	Gene name	Fold change	ANOVA*
Downregulated proteins						
Proteins involved in antioxidant process						
1	62,957/5.8	Putative cysteine ligase BshC	Q6GHQ8	bshC	1.67423	0.002095
2	20,977/4.9	Alkyl hydroperoxide reductase C	Q6GJR7	ahpC	1.43582	0.018934
3	18,005/4.6	Thiol peroxidase	Q8NW51	tpx	1.40798	0.028300
4	16,207/4.6	UPF0403 protein SAR1592	Q6GGI4	SAR1592	4.98156	0.018337
5	18,627/4.7	UPF0312 protein MW2606	Q8NUH6	MW2606	1.45493	0.00837
Stress associated proteins						
6	15,165/5.2	Urease subunit beta	Q8NV90	ureB	1.69159	0.007651
7	18,475/5.6	Putative universal stress protein MW1653	Q7A0N0	MW1653	1.33193	0.020852
Proteins associated with purine metabolism						
8	19,117/4.8	Adenine phosphoribosyltransferase	P68781	apt	2.40972	$4.82E^{-04}$
9	21,403/4.9	dITP/XTP pyrophosphatase	P58995	MW1034	2.65243	$1.71E^{-04}$
10	24,513/5.0	Phosphoribosylformylglycinamidine synthase subunit PurQ	Q6GI16	purQ	2.15662	0.014347
Biofilm and virulence associated proteins						
11	17,482/4.6	Low molecular weight protein-tyrosine-phosphatase PtpA	Q6GFH6	ptpA	1.1288	0.043825
12	15,788/5.0	Low molecular weight protein-tyrosine-phosphatase PtpB	Q7A0B9	ptpB	2.57108	0.004072
13	42,057/4.9	Succinate–CoA ligase [ADP-forming] subunit beta	P66872	sucC	1.20415	$4.50E^{-04}$
14	113,619/4.6	Fibronectin-binding protein A	A7X6I5	fnbA	1.4588	0.033728
15	26,680/5.2	2,3-bisphosphoglycerate-dependent phosphoglycerate mutase	P65709	gpmA	2.22576	0.003304
16	7019/5.2	UPF0337 protein MW0793	Q7A1E3	MW0793	1.24105	0.001998
17	18,186/9.7	Protein SprT-like	P67728	MW1986	1.24428	0.038033
Other critical proteins						
18	24,595/5.1	Cytidylate kinase	P63807	cmk	1.6239	0.015647
19	22,490/5.4	HTH-type transcriptional regulator SAR2658	Q6GDM3	SAR2658	1.10477	0.045022
20	17,920/4.8	Serine-protein kinase RsbW	Q8NVI5	rsbW	1.26239	0.015755
21	17,238/4.8	Transcriptional regulator MraZ	Q6GHQ7	mraZ	2.07428	0.004743
22	14,844/5.6	ATP synthase epsilon chain	Q6GEX3	atpC	1.91606	0.002441
23	29,095/5.4	30S ribosomal protein S2	Q6GHH9	rpsB	3.97255	0.022209
24	19,145/4.8	Ribosome maturation factor RimM	Q6GHJ6	rimM	1.20018	0.047695
25	19,073/4.9	Ribosome maturation factor RimM	P66657	rimM	1.30272	0.05898
26	44,591/5.7	Staphopain B	Q6GI35	sspB	1.60676	0.018606
27	38,769/5.1	Isopentenyl-diphosphate delta-isomerase	Q8NV55	fni	1.35708	0.044001
28	37,027/5.4	tRNA uridine (34) hydroxylase	Q8NUH3	trhO	1.40007	0.002195
29	33,482/5.1	GTP cyclohydrolase FolE2	Q8NXX2	folE2	1.98712	$9.61E^{-04}$
30	33,293/5.3	Arginase	Q8NVE3	arg	1.63518	0.02596
31	44,996/5.6	UDP-N-acetylglucosamine 1-carboxyvinyltransferase 1	Q6GEX5	murA1	1.91077	0.006293
32	22,119/5.8	Putative acetyltransferase MW2476	Q8NUR1	MW2476	1.69156	0.004024
33	17,002/4.9	Uncharacterized N-acetyltransferase MW1059	Q7A135	MW1059	1.24634	0.016056
34	30,975/4.8	Uncharacterized hydrolase SAR2661	Q6GDM0	SAR2661	1.40615	$2.70E^{-05}$
35	23,333/5.0	FMN-dependent NADH-azoreductase	Q6GKA4	azoR	2.53591	0.008689
36	29,449/4.9	Uncharacterized protein MW1299	Q7A0W8	MW1299	1.68461	0.048214
37	24,577/5.0	Uncharacterized oxidoreductase MW2403	Q8NUV9	MW2403	1.82239	$2.41E^{-04}$
38	62,428/5.8	Phosphoglucomutase	Q8NUV4	pgcA	3.2874	$2.38E^{-04}$
Upregulated proteins						
39	23,502/4.6	Deoxyribose-phosphate aldolase 1	Q6GKG7	deoC1	4.00713	0.001501
40	22,104/5.6	Probable nicotinate-nucleotide adenylyltransferase	P65503	nadD	1.11072	0.035087

*p value less than 0.05 is statistically significant

Fig. 2 Interacting protein partners of differentially regulated proteins, predicted through STRING database. Colored nodes represent the query proteins and the first shell of interactors; white nodes represent the second shell of interactors. Line thickness indicates the degree of confidence prediction of the interaction

Downregulated proteins were mainly linked with biofilm and virulence production.

Proteins Associated with Antioxidant Systems

Thiol peroxidase (Tpx) protein was downregulated with a fold change of 1.4 ($p = 0.02$) during docosanol treatment. In general, Trx and Grx are the major antioxidant systems that confer resistance under oxidative stress. However, Grx antioxidant system is absent in many Gram-positive bacteria including *Bacillus* spp. and *S. aureus*, consequently making Trx the substantial antioxidant system to maintain the cellular redox homeostasis. Instead of Grx, *S. aureus* possesses an alternative low molecular weight thiol system Brx [30]. The primary function of Brx is to maintain the reduced state of the cell as well as the detoxification of reactive oxygen, nitrogen and electrophilic species, antibiotics and alkylating agents [11, 31, 32].

Protein BshC (putative cysteine ligase in bacillithiol production) and BrxA (bacilliredoxin) were downregulated with a fold change of 1.6 ($p = 0.002$) and 4.9 ($p = 0.01$), respectively in docosanol treatment. BSH synthesis is induced in response to oxidative stress mounted by neutrophils or macrophages of the host system during infection [33, 34]. Generally, three genes are involved in the production of BSH namely *bshA*, *bshB*, and *bshC* [35]. Pöther et al. [36] reported that BSH producing strains are more resistant to antibiotic fosfomycin and sodium hypochlorite than BSH-negative strains. In addition, the bacterial load in upper-airway epithelial cells and murine macrophages was significantly disrupted in the BSH-negative strain. Whereas the CFU load was comparatively higher in BSH producing strains. Similarly, a mutation in *bshA* and *bshC* has been shown to significantly affect the survival rate of *S. aureus* in human whole-blood, independent of other enzymes [34]. The present study's findings (spotted through proteomics profiling data) were congruent with previous report of docosanol on human whole-blood survival assay [13]. Thus, down-regulation of BshC strengthens the viewpoint on BSH production and *S. aureus* survival.

Alkyl hydroperoxide reductase C (AhpC) protein was found to downregulated with a fold change of 1.4 ($p = 0.02$) during docosanol treatment. Alkyl hydroperoxide peroxidase takes part in the antioxidant process to detoxify the organic hydroperoxide, by transferring electrons to AhpC. Several studies are describing the production of *ahpC* in all-time points of biofilm and their virulence properties through in vivo studies [37]. Notably, docosanol treatment in MRSA reduced the expression of AhpC to 1.4 fold.

Acidic Stress Associated Proteins

The protein urease subunit B (UreB), part of the urea degradation pathway, was found to be downregulated with a fold change of 1.6 ($p = 0.007$) during docosanol treatment. When *S. aureus* is grown in excess glucose concentration, it produces acetate through pyruvate and potentiates cell death by presenting a low pH environment. In order to thrive in such acidic conditions, *S. aureus* produces ammonia through the urease cycle, which neutralize the effect of low pH and

protect itself from the acidic environment. It has also been reported that genes associated with the urease cycle are highly transcribed during biofilm development. The importance of urease in establishing persistent chronic renal infection in the murine models has been reported by Zhou et al. [38]. Hence, downregulation of UreB is envisaged to be associated with biofilm development.

Proteins Associated with Purine Metabolism

Adenine phosphoribosyltransferase (Apt) which catalyses the formation of AMP from adenine in the purine salvage pathway was found to be downregulated with a fold change of 2.4 ($p < 0.001$) during docosanol treatment. Besides, pyrophosphatases which catalyse the hydrolysis of non-standard nucleotides such as dITP (deoxyinosine triphosphate), XTP (xanthosine triphosphate), and ITP (inosine triphosphate) to their corresponding monophosphate derivatives (IMP and XMP), in order to avoid the incorporation of non-standard purine nucleotides into DNA/RNA, was found to be downregulated with a fold change of 2.6 ($p < 0.001$) [39]. Also, Phosphoribosylformylglycinamidine synthase subunit PurQ involved in the purine biosynthetic pathway was downregulated with a fold change of 2.1 ($p = 0.01$). PurQ converts glutamine to glutamate to generate ammonia [40]. Altogether, the downregulation of essential proteins such as Apt, PurQ, and pyrophosphatase from purine pathways indicates that docosanol targets the purine metabolic pathway in MRSA.

Biofilm and Virulence-Associated Proteins

Staphylococcus aureus secretes two low molecular weight phosphotyrosine protein phosphatases, viz. PtpA and PtpB, which dephosphorylate the tyrosyl phosphorylated protein. Protein PtpA is secreted during macrophage infection and thus deletion of *ptpA* gene in *S. aureus* affects intramacrophage survival and infectivity [41]. Here, docosanol treatment reduced the expression of both PtpA and PtpB to 1.1 and 2.5 fold, respectively. Succinyl-coenzyme A synthetase (sucC), a gene that has been reported to be highly expressed under biofilm conditions [42, 43] was found to be downregulated in docosanol-treated samples.

Despite the role of FnbpA in adherence and biofilm formation in vitro conditions, in vivo studies have revealed the indispensable role of FnbpA in biofilm development [44]. It plays a critical role in the accumulation phase of biofilm development and host cell infection [45, 46]. In this study, docosanol downregulated the expression of FnbpA with a fold change of 1.4 ($p = 0.03$).

Remarkably, docosanol treatment down-regulated the GpmA expression (2.2 fold, $p = 0.003$) in MRSA. *S. aureus* has two variants of phosphoglycerate mutase viz. GpmI (a primary enzyme, Mn-dependent) and GpmA (Mn-independent). During infection, *S. aureus* utilizes glucose as the primary carbon source through the glycolytic pathway. In order to obstruct the pathogen from utilizing glucose molecules, host defence pathways limits the metal availability for glycolytic substrate and phosphoglycerate mutase, by producing metal-chelating proteins (particularly, Mn-binding calprotectin) through a process termed nutritional immunity [47]. However, *S. aureus* has the other variant (GpmA, Mn-independent) to overcome the metal-starvation stress. It is a common strategy not restricted to *S. aureus* but also to other Gram-positive as well as Gram-negative bacteria to survive in the metal-deficit host environment. Furthermore, Δ*gpmA* mutant sensitizes *S. aureus* to calprotectin while Δ*gpmI* mutant has no signficant effect. Sensitivity is reversed when a plasmid encoding *gpmA* gene is expressed in Δ*gpmA*. Thus, *gpmA* is critical to resist nutritional immunity in order to maintain the glycolytic flux as well as for establishing the infection in the host cell during metal-starvation [48].

Other Critical Proteins

Cytidylate kinase encoded by *cmk* was downregulated with a fold change of 1.6 ($p = 0.01$) during docosanol treatment. Cytidylate monophosphate (CMP) kinase, belonging to the nucleoside monophosphate kinase family, catalyses the transfer of phosphate group from ATP to CMP. It is involved in nucleoside precursor synthesis and is essential for survival. Blocking of CMP kinase with antisense peptide nucleic acid demonstrates antibacterial activity against *S. aureus*. The essentiality of CMP kinase in survival has also been validated through in vivo studies in which the bacterial load was significantly reduced in antisense peptide nucleic acid-treated mice [49]. In addition, the HTH-transcriptional regulator, a DNA-binding protein that either activates or represses the wide spectrum of virulence genes [50], was downregulated (fold change: 1.1, $p = 0.04$). RsbW, a negative regulator of SigB [51], from *sigB* operon was downregulated (fold change: 1.2, $p = 0.01$) in docosanol treatment. Besides, a cell division protein MraZ [52] was found to be down-regulated (fold change: 2.0, $p = 0.004$) in docosanol treatment.

ATP synthase epsilon chain (AtpC) protein expression was downregulated in docosanol treatment with a fold change of 1.9 ($p = 0.002$). It is encoded by *atpC* gene and is a component of ATP synthase, involved in generating ATP. A small-molecule diarylquinoline, a class of antibacterial agents, is reported to eradicate the biofilm in *S. aureus* by blocking the function of ATP synthase [53]. The present findings correlate well with the findings of Balemans et al. [53].

Proteins such as RpsB, RimM, YceI (MW2606), and MW1653 was downregulated with a fold change of 3.9 ($p = 0.02$), 1.2 ($p = 0.04$), 1.4 ($p = 0.00$), and 1.3 ($p = 0.02$),

A. BIOLOGICAL PROCESS
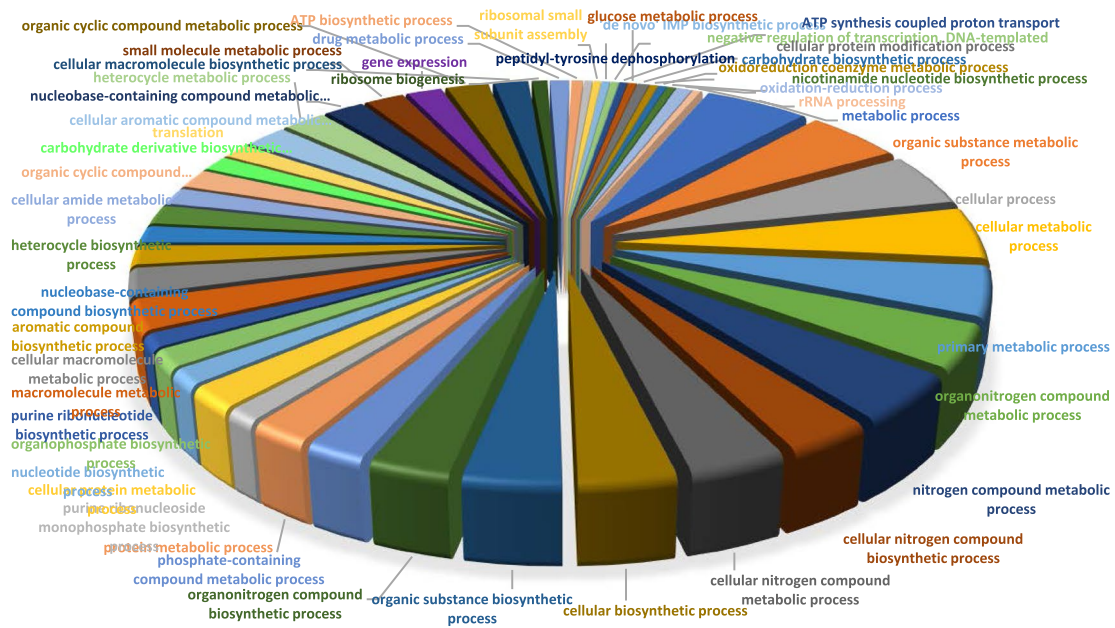
B. MOLECULAR FUNCTION
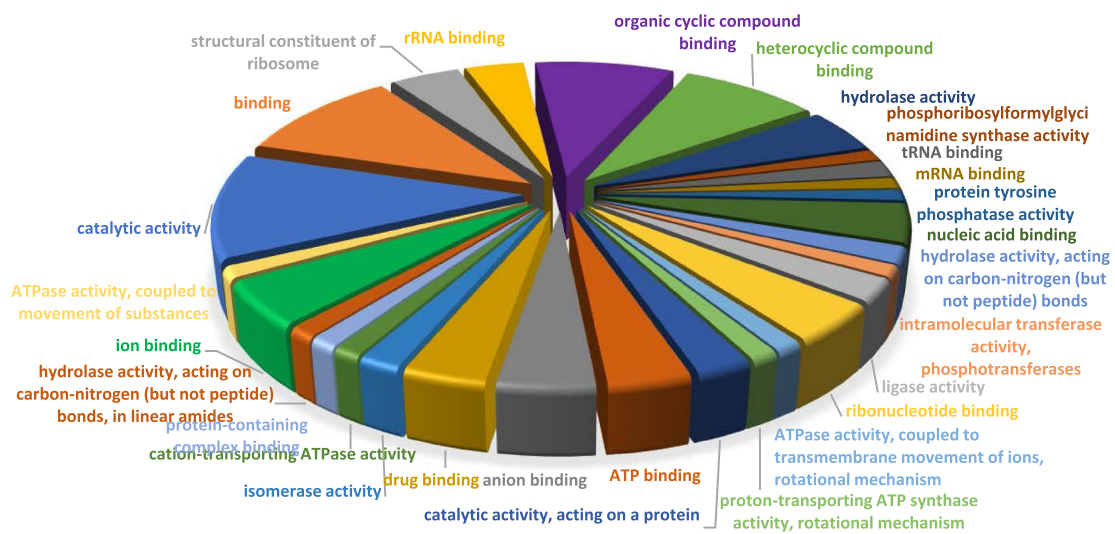
C. CELLULAR COMPONENTS
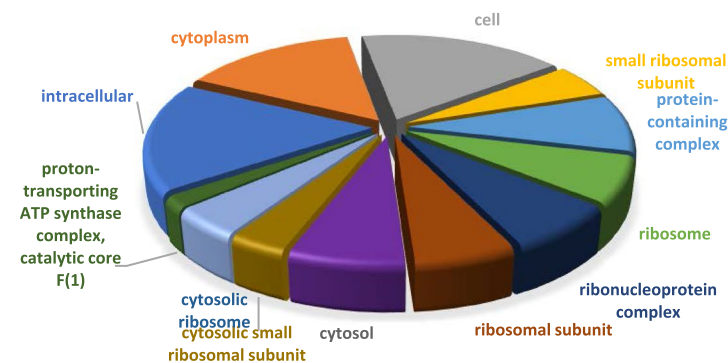
◄**Fig. 3** Gene ontology (GO) analysis of differentially regulated proteins. Pie charts representing three GO categories. **A** Biological processes, **B** molecular function and **C** cellular component

respectively during docosanol treatment. It has also been observed that cells in the biofilm state experience more stress response than the cells in the planktonic state. Ribosomal proteins are also reported to be highly expressed during biofilm formation [42, 54]. Despite the role in protein translation, recent studies on the interaction of positively charged ribosomal proteins with anionic cell wall components indicate the defensive mechanism in response to challenges from host response or antibiotics [54]. Significant downregulation of ribosomal and stress proteins evidences the antibiofilm efficacy of docosanol and these findings are in accordance with physiological assays from the previous report [13].

Staphopain B, a cysteine protease that inhibits the host's innate immune response [55], was downregulated with a fold change of 1.6 ($p = 0.01$). Besides, isopentenyl-diphosphate delta isomerase (involved in isoprenoid biosynthesis), tRNA uridine [34] hydroxylase (tRNA undergoes chemical modification at 34th position to promote efficient decoding process during protein synthesis) [56], GTP cyclohydrolase (involved in folate biosynthesis pathway) [57], arginase (RocF, arginine biosynthesis pathway) [58] and UDP-*N*-acetylglucosamine 1-carboxyvinyltransferase 1 (involved in cell wall formation [59]) were downregulated.

The uncharacterized proteins that were differentially regulated during docosanol treatment in *S. aureus* were identified through comparative modeling and the list is given in Table 2. In case of uncharacterized proteins that have no structural homologs in the PDB database were identified through sequence homology and conserved domain database.

YjbJ

Nakamura et al. [60], while studying the extended-spectrum β-lactamase producing multidrug-resistant *E. coli* sequence type 131 (ESBL- *E. coli* ST131), identified five proteins such as YahO, YjbJ, YnfD, acid resistance chaperone protein HdeA and cytochrome b562 with specific amino acid substitution responsible for higher prevalence of drug resistance and postulated that YjbJ (a stress-induced protein) interaction with YahO might be associated with biofilm formation. Also, they identified amino acid substitutions of Val59 to Asp59, Asp60 to Ser60, and Thr63 to Lys63 were found to be prevalent among YjbJ protein of ST131. Here, the uncharacterized *S. aureus* UPF0337 protein MW0793 was identified as YjbJ, and the reported amino acid substitutions were located in *S. aureus* YjbJ through pairwise sequence alignment (Fig. 4). Interestingly, semi conservation of Val to

Table 2 Structural and functional insight into uncharacterized proteins that were differentially regulated during docosanol treatment in MRSA, through comparative modelling technique

S. aureus accession number	Protein name	Homologous organism/ accession number	% of similarity between structural homologs	Gene name	Predicted function	References
Q7A1E3	UPF0337 protein MW0793	*Escherichia coli* (strain K12)/P68206	42	*yjbJ* (CsbD domain)	Biofilm formation	Pineda-Lucena et al. [71]
Q6GGI4	UPF0403 protein SAR1592	*Bacillus subtilis* (strain 168)/P54170	52.8	*brxA* (bacilliredoxin, BrxA/ BrxB family)	Oxidative stress	Derewenda et al. [72]
Q8NUH6	UPF0312 protein MW2606	-	-	*yceI* (Putative periplasmic polyisoprenoid binding protein)	Oxidative stress	Stancik et al. [65] and Weber et al. [66]
P67728	MW1986	-	-	Zinc containing metalloproteases (protein SprT-like)	Virulence determinant	Miyoshi and Shinoda [67]
Q8NUR1	Putative acetyltransferase MW2476	Putative acetyltransferase SACOL2570/Q5HCZ5	100	Galactoside *O*-acetyltransferase	Detoxification process and resistance	Luo et al. [69]
Q7A135	Uncharacterized *N*-acetyltransferase MW1059	*Bacillus subtilis*/Q34468	45.3	*ylbP, N*-acetyltransferase	Detoxification process and resistance	Evans [73]
Q7A0N0	Putative universal stress protein MW1653	*Lactobacillus plantarum*/F9UMW3	35.51	Universal stress protein	Protective effect during stress stimuli	Tkaczuk et al. [74]

Proteins that have no structural homologs in PDB database (indicated in hyphen sign) were identified through sequence homology and conserved domain database

```
S.aureus      ---MADESKFEQAKGNVKETVGNVTDNKNLENEGKEDKASGKAKEFVENAKEKATD-FID    56
E.coli_yjbJ   MNKDEAGGNWKQFKGKVKEQWGKLTDDDMTIIEGKRDQLVGKIQERYGYQKDQAEKEVVD    60
              .:::* **:*** *:.**:.    ***.*: ** :*    *::* . .:*

S.aureus      KVKGNKGE-    64
E.coli_yjbJ   WETRNEYRW    69
              .  *:  .
```
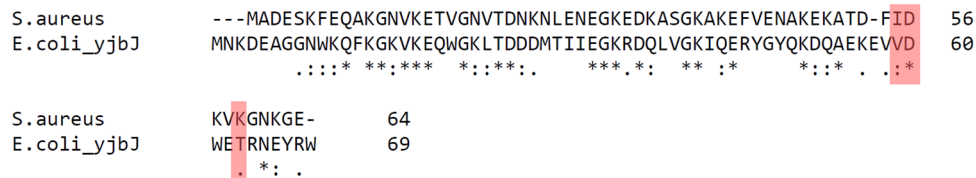
Fig. 4 Pairwise sequence alignment showing YjbJ protein sequence from *S. aureus* and *E. coli*. Red bars represent the specific amino acid substitution, responsible for higher prevalence of drug resistance in *E. coli*

Ile and conservation of Thr to Lys mutation were observed in *S. aureus* YjbJ. However, the actual function associated with YjbJ in *S. aureus* needs to be studied in detail.

BrxA

Based on sequence and structural homology, UPF0403 protein SAR1592 in *S. aureus* was identified to be thiol-disulfide oxidoreductase BrxA [61], which is considered to be involved in balancing the intracellular oxidative stress. This novel bacilliredoxin contains CGC as a highly conserved motif (belongs to DUF1094 family) and this feature distinguishes them from the thioredoxin which contains CXXC as a highly conserved motif [62, 63]. The role of bacilliredoxin in vivo through the fusion of *S. aureus* Brx and roGFP2 has been reported [64].

YceI

UPF0312 protein MW2606 shows 33.3% similarity with YceI from *Campylobacter jejuni*. The gene encoding *yceI* is a poly isoprenoid binding periplasmic membrane protein, expressed in high pH conditions and induced under osmotic stress in *E. coli* [65, 66]. However, the YceI function in *S. aureus* needs to be explored (Fig. 5).

Zinc-Containing Metalloprotease

Zinc-containing metalloproteases are reported to digest a wide range of host proteins. They are produced by opportunistic human pathogens and are considered to be a lethal factor. Zinc-metalloprotease in particular metzincins shares HEXXHXXGXXH as a consensus motif with His at places one, five, and eleven. However, *S. aureus* has HEXXHXXXXXXXXGXXH as a consensus motif with His at places one, five, and seventeen. Here, the position of His residue indicates the location of the zinc ligand [67]. Interestingly, the position of the fifth zinc ligand (Tyr) was retained at the 41st position in *S. aureus* (Fig. 6), which is a characteristic feature of the serralysin family (SXMSY). However, Met at 39th position of serralysin was found to be replaced with Glu in *S. aureus*. Notably, other homologs of spr-T like zinc-containing metalloprotease from *Bacillus*

and *Staphylococcus* spp. (which shares > 48% similarity with spr-T like zinc-containing metalloprotease of *S. aureus*), was found to be replaced with other amino acids (Fig. 6).

N-Acetyltransferase and Galactoside *O*-Acetyltransferase

Acetyltransferase transfers the acetyl group from a wide variety of substrates including aminoglycoside antibiotics in pathogenic bacteria [68]. Galactoside O-acetyltransferase (GAT), also known as thiogalactosidetransacetylase, is one of the proteins from human pathogens that come under the National Institute for Allergy and Infectious Diseases (NIAID) Category A–C priority lists and it is mainly associated with toxin production and antibiotic resistance through detoxification process [69]. *S. aureus* treated with an antibiotic fusidic acid has been shown to downregulate the GAT gene [70]. Structures of uncharacterized proteins and their respective templates along with QMQE scores are shown in Fig. S1 and Table 3, respectively. The modelled structure was deposited in the protein model database (PMDB) and their corresponding Id is given in Table S1.

Lakshmi et al. [13] have shown downregulation of *fnbA* gene through RT-PCR analysis and the result is consistent with the downregulation of fnbA proteins in the current study. Besides, most of the downregulated proteins in this study were associated with biofilm development and antioxidant system. These results are supported by biofilm inhibition and H_2O_2 assays, respectively [13]. In addition, reduced protein expression of BshA was in accordance with decreased survival of MRSA in human whole-blood survival assay [34], as reported by Lakshmi et al. [13].

Conclusion

S. aureus encounters redox modulators such as ROS, reactive nitrogen species (RNS), and reactive sulphur species (RSS) by the host immune system during infection and antibiotic treatment. However, it utilizes thiol-based redox sensors (brxA, brxB, and ypdA) to overcome oxidative stress. Intriguingly, the study attempted to find the mechanism of docosanol against MRSA revealed bacillithiol as the chief

Fig. 5 Interaction partners of BshR. **A** Interaction partner predicted through STRING database and **B** gene co-occurrence analysis
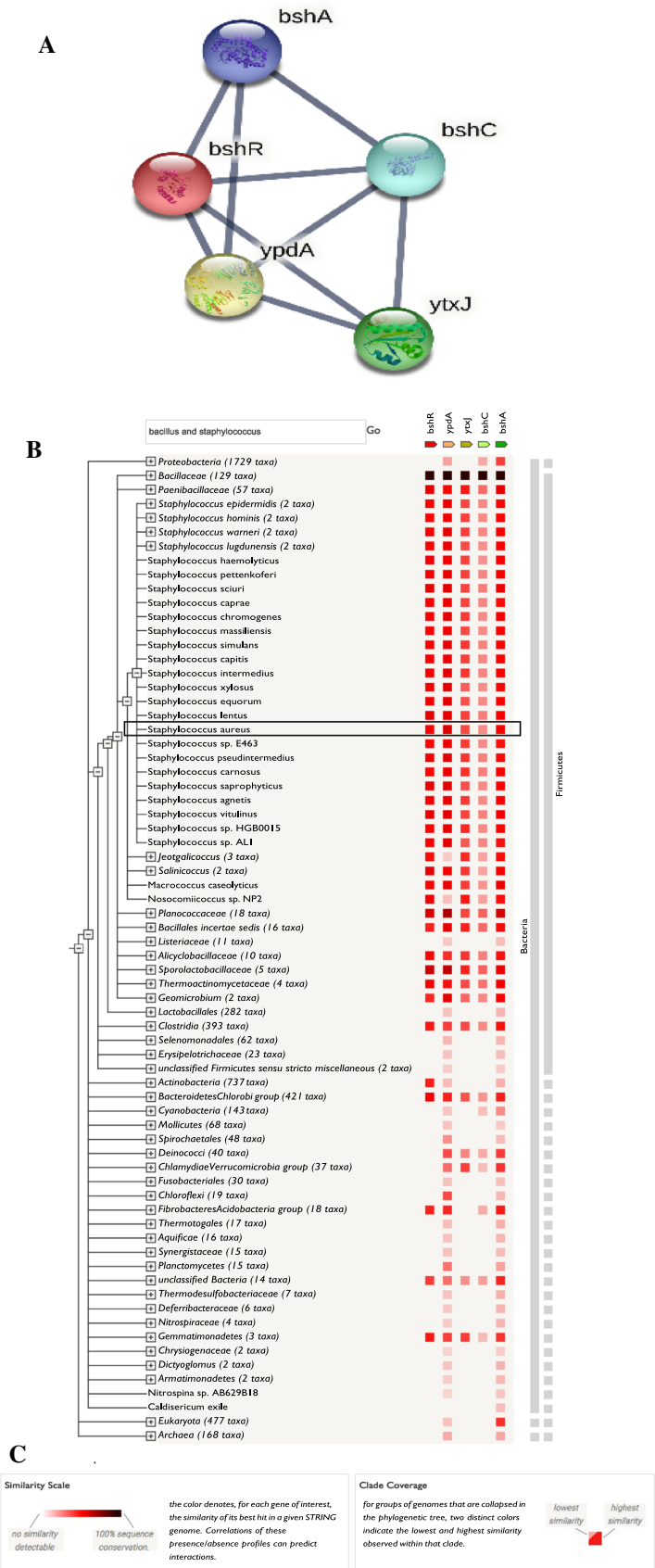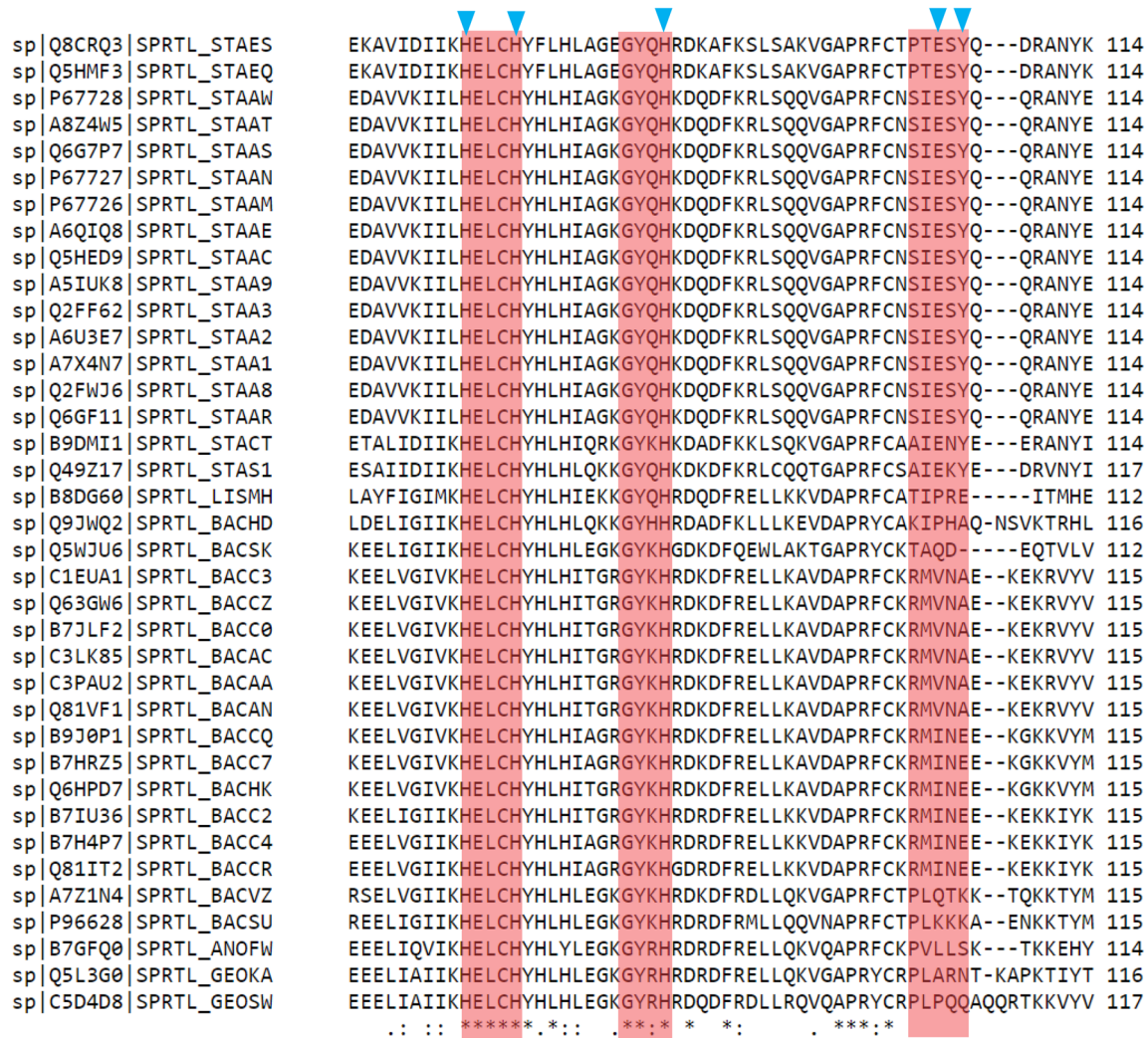
Fig. 6 Multiple sequence alignment of spr-T like zinc-containing metalloprotease sequence from *Bacillus* and *Staphylococcus* spp. Conserved regions and residues are highlighted in red box and blue triangles, respectively

Table 3 List of uncharacterized proteins showing their respective templates and GMQE score

S. no.	Protein	Template PDB ID	GMQE score
1	YjbJ	1RYK	0.63
2	BrxA	3FHK	0.81
3	YlbP	2PR1	0.79
4	Metalloprotease MW1986	6MDX	0.46
5	GAT	3FTT	0.89
6	Universal stress protein	3S3T	0.49

target. In addition, it reduced the expression of critical proteins that are essential for biofilm formation and virulence production. Targeting redox-based system such as bacillithiol is an emerging field of study to combat multi-drug resistance in *S. aureus*. Therefore, the present work gathers insights into the drugs that target redox stress conditions. However, the efficacy of docosanol could be made more explicit by examining their activity in other clonal complexes of MRSA. In the case of uncharacterized proteins, further experiments are required to support the predicted functions.

Declarations

References

1. Hampton, T. (2016). First-line antibiotics may worsen MRSA infection. *JAMA, 315*, 19.

2. McConoughey, S. J., Howlin, R., Granger, J. F., Manring, M. M., Calhoun, J. H., Shirtliff, M., Kathju, S., & Stoodley, P. (2014). Biofilms in periprosthetic orthopedic infections. *Future Microbiology, 9*, 987–1007.

3. El-Ganiny, A. M., Shaker, G. H., Aboelazm, A. A., & El-Dash, H. A. (2017). Prevention of bacterial biofilm formation on soft contact lenses using natural compounds. *The Journal of Ophthalmic Inflammation and Infection, 7*, 11.

4. Geremias, T. C., Montero, J. F. D., Magini, R. S., Schuldt Filho, G., de Magalhaes, E. B., & Bianchini, M. A. (2017). Biofilm analysis of retrieved dental implants after different peri-implantitis treatments. *Case Reports in Dentistry, 2017*, 8562050.

5. Gomes, A., van Oosten, M., Bijker, K. L. B., Boiten, K. E., Salomon, E. N., Rosema, S., Rossen, J. W. A., Natour, E., Douglas, Y. L., Kampinga, G. A., van Assen, S., & Sinha, B. (2018). Sonication of heart valves detects more bacteria in infective endocarditis. *Science and Reports, 8*, 12967.

6. Thorarinsdottir, H. R., Kander, T., Holmberg, A., Petronis, S., & Klarin, B. (2020). Biofilm formation on three different endotracheal tubes: A prospective clinical trial. *Critical Care, 24*, 382.

7. Painter, K. L., Strange, E., Parkhill, J., Bamford, K. B., Armstrong-James, D., & Edwards, A. M. (2015). *Staphylococcus aureus* adapts to oxidative stress by producing H2O2-resistant small-colony variants via the SOS response. *Infection and Immunity, 83*, 1830–1844.

8. Pavelescu, L. A. (2015). On reactive oxygen species measurement in living systems. *The Journal of Medicine and Life, 8*, 38–42.

9. Paiva, C. N., & Bozza, M. T. (2014). Are reactive oxygen species always detrimental to pathogens? *Antioxidants & Redox Signaling, 20*, 1000–1037.

10. Beavers, W. N., & Skaar, E. P. (2016). Neutrophil-generated oxidative stress and protein damage in *Staphylococcus aureus*. *Pathogens and Disease, 74*, ftw060.

11. Lu, J., & Holmgren, A. (2014). The thioredoxin antioxidant system. *Free Radical Biology & Medicine, 66*, 75–87.

12. Liao, X., Yang, F., Li, H., So, P. K., Yao, Z., Xia, W., & Sun, H. (2017). Targeting the thioredoxin reductase-thioredoxin system from *Staphylococcus aureus* by silver ions. *Inorganic Chemistry, 56*, 14823–14830.

13. Lakshmi, S. A., Bhaskar, J. P., Krishnan, V., Sethupathy, S., Pandipriya, S., Aruni, W., & Pandian, S. K. (2020). Inhibition of biofilm and biofilm-associated virulence factor production in methicillin-resistant *Staphylococcus aureus* by docosanol. *Journal of Biotechnology, 317*, 59–69.

14. Seidl, K., Goerke, C., Wolz, C., Mack, D., Berger-Bächi, B., & Bischoff, M. (2008). *Staphylococcus aureus* ccpA affects biofilm formation. *Infection and Immunity, 76*, 2044–2050.

15. Molière, N., & Turgay, K. (2009). Chaperone-protease systems in regulation and protein quality control in *Bacillus subtilis*. *Research in Microbiology, 160*, 637–644.

16. Valliammai, A., Sethupathy, S., Ananthi, S., Priya, A., Selvaraj, A., Nivetha, V., Aravindraja, C., Mahalingam, S., & Pandian, S. K. (2020). Proteomic profiling unveils citral modulating expression of IsaA, CodY and SaeS to inhibit biofilm and virulence in methicillin-resistant *Staphylococcus aureus*. *International Journal of Biological Macromolecules, 29*, 208–221.

17. ruger N.J. (2009). The Bradford method for protein quantitation. In J. M. Walker (Ed.), *The protein protocols handbook* (pp. 17–24). Humana Press, Totowa: Springer Protocols Handbooks.

18. Sianglum, W., Srimanote, P., Wonglumsom, W., Kittiniyom, K., & Voravuthikunchai, S. P. (2011). Proteome analyses of cellular proteins in methicillin-resistant *Staphylococcus aureus* treated with rhodomyrtone, a novel antibiotic candidate. *PLoS ONE, 6*, e16628.

19. Prasath, K. G., Sethupathy, S., & Pandian, S. K. (2019). Proteomic analysis uncovers the modulation of ergosterol, sphingolipid and oxidative stress pathway by myristic acid impeding biofilm and virulence in *Candida albicans*. *Journal of Proteomics., 208*, 103503.

20. Bienvenut, W. V., Déon, C., Pasquarello, C., Campbell, J. M., Sanchez, J.-C., Vestal, M. L., & Hochstrasser, D. F. (2002). Matrix-assisted laser desorption/ionization-tandem mass spectrometry with high resolution and sensitivity for identification and characterization of proteins. *Proteomics, 2*, 868.

21. Szklarczyk, D., Gable, A. L., Nastou, K. C., Lyon, D., Kirsch, R., Pyysalo, S., Doncheva, N. T., Legeay, M., Fang, T., Bork, P., Jensen, L. J., & von Mering, C. (2021). The STRING database in 2021: customizable protein–protein networks, and functional characterization of user-uploaded gene/measurement sets. *Nucleic Acids Research, 49*, D605–D612.

22. Lakshmi, S. A., Shafreen, R. B., Priyanga, A., Shiburaj, S., & Pandian, S. K. (2020). A highly divergent α-amylase from *Streptomyces* spp.: An evolutionary perspective. *International Journal of Biological Macromolecules, 163*, 2415–2428.

23. Zhang, L., Wen, Q., Mao, H. P., Luo, N., Rong, R., Fan, J. J., & Yu, X. Q. (2013). Developing a reproducible method for the high-resolution separation of peritoneal dialysate proteins on 2-D gels. *Protein Expression and Purification, 89*, 196–202.

24. Monteiro, R., Vitorino, R., Domingues, P., Radhouani, H., Carvalho, C., Poeta, P., et al. (2012). Proteome of a methicillin-resistant *Staphylococcus aureus* clinical strain of sequence type ST398. *Journal of Proteomics, 75*, 2892–2915.

25. Shamsuddin, N. A. M., Basri, D. F., Zin, N. M., Raus, A. R., & Bakar, N. F. A. (2021). Analysis of two-dimensional gel electrophoresis map of methicillin-resistant *Staphylococcus aureus* treated with acetone extract from *Canarium odontophyllum* Miq. leaves. *American Journal of Plant Sciences, 12*, 37–52.

26. Azmi, K., Qrei, W., & Abdeen, Z. (2019). Screening of genes encoding adhesion factors and biofilm production in methicillin resistant strains of *Staphylococcus aureus* isolated from Palestinian patients. *BMC Genomics, 20*, 1–12.

27. Arce Miranda, J. E., Sotomayor, C. E., Albesa, I., & Paraje, M. G. (2011). Oxidative and nitrosative stress in *Staphylococcus aureus* biofilm. *FEMS Microbiology Letters, 315*, 23–29.

28. Gélinas, M., Museau, L., Milot, A., & Beauregard, P. B. (2020). Cellular adaptation and the importance of the purine biosynthesis pathway during biofilm formation in Gram-positive pathogens. *bioRxiv.* https://doi.org/10.1101/2020.12.11.422287

29. De Backer, S., Sabirova, J., De Pauw, I., De Greve, H., Hernalsteens, J. P., Goossens, H., & Malhotra-Kumar, S. (2018). Enzymes catalyzing the TCA-and urea cycle influence the matrix composition of biofilms formed by methicillin-resistant *Staphylococcus aureus* USA300. *Microorganisms, 6*, 113.

30. Gaballa, A., Chi, B. K., Roberts, A. A., Becher, D., Hamilton, C. J., Antelmann, H., & Helmann, J. D. (2014). Redox regulation in *Bacillus subtilis*: The bacilliredoxins BrxA (YphP) and BrxB (YqiW) function in de-bacillithiolation of S-bacillithiolated OhrR and MetE. *Antioxidants & Redox Signaling, 21*, 357–367.

31. Chandrangsu, P., Loi, V. V., Antelmann, H., & Helmann, J. D. (2018). The role of bacillithiol in Gram-positive firmicutes. *Antioxidants & Redox Signaling, 28*, 445–462.

32. Newton, G. L., Fahey, R. C., & Rawat, M. (2012). Detoxification of toxins by bacillithiol in *Staphylococcus aureus*. *Microbiology, 158*, 1117–1126.

33. Linzner, N., Vu, L. V., Fritsch, V. N., Tung, N., Stenzel, S., Wirtz, M., Hell, R., Hamilton, C. J., Tedin, K., Fulde, M., & Antelmann, H. (2019). *Staphylococcus aureus* uses the bacilliredoxin (BrxAB)/bacillithioldisulfide reductase (YpdA) pathway to defend against oxidative stress under infections. *Frontiers in Microbiology, 10*, 1355.

34. Posada, A. C., Kolar, S. L., Dusi, R. G., Francois, P., Roberts, A. A., Hamilton, C. J., Liu, G. Y., & Cheung, A. (2014). Importance of bacillithiol in the oxidative stress response of *Staphylococcus aureus*. *Infection and Immunity, 82*, 316–332.

35. Gaballa, A., Newton, G. L., Antelmann, H., Parsonage, D., Upton, H., Rawat, M., Claiborne, A., Fahey, R. C., & Helmann, J. D. (2010). Biosynthesis and functions of bacillithiol, a major low-molecular-weight thiol in Bacilli. *Proceedings of the National academy of Sciences of the United States of America, 107*, 6482–6486.

36. Pöther, D. C., Gierok, P., Harms, M., Mostertz, J., Hochgrafe, F., Antelmann, H., Hamilton, C. J., Borovok, I., Lalk, M., Aharonowitz, Y., & Hecker, M. (2013). Distribution and infection-related functions of bacillithiol in *Staphylococcus aureus*. *International Journal of Medical Microbiology, 303*, 114–123.

37. Cosgrove, K., Coutts, G., Jonsson, I. M., Tarkowski, A., Kokai-Kun, J. F., Mond, J. J., & Foster, S. J. (2007). Catalase (KatA) and alkyl hydroperoxide reductase (AhpC) have compensatory roles in peroxide stress resistance and are required for survival, persistence, and nasal colonization in *Staphylococcus aureus*. *Journal of Bacteriology, 189*, 1025–1035.

38. Zhou, C., Bhinderwala, F., Lehman, M. K., Thomas, V. C., Chaudhari, S. S., Yamada, K. J., Foster, K. W., Powers, R., Kielian, T., & Fey, P. D. (2019). Urease is an essential component of the acid response network of *Staphylococcus aureus* and is required for a persistent murine kidney infection. *PLoS Pathogens, 15*, e1007538.

39. Burgis, N. E., & Cunningham, R. P. (2007). Substrate specificity of RdgB protein, a deoxyribonucleoside triphosphate pyrophosphohydrolase. *Journal of Biological Chemistry, 282*, 3531–3538.

40. Zhang, Y., Morar, M., & Ealick, S. E. (2008). Structural biology of the purine biosynthetic pathway. *Cellular and Molecular Life Sciences, 65*, 3699–3724.

41. Gannoun-Zaki, L., Patzold, L., Huc-Brandt, S., Baronian, G., Elhawy, M. I., Gaupp, R., Martin, M., Blanc-Potard, A. B., Letourneur, F., Bischoff, M., & Molle, V. (2018). PtpA, a secreted tyrosine phosphatase from *Staphylococcus aureus*, contributes to virulence and interacts with coronin-1A during infection. *Journal of Biological Chemistry, 293*, 15569–15580.

42. Resch, A., Rosenstein, R., Nerz, C., & Gotz, F. (2005). Differential gene expression profiling of *Staphylococcus aureus* cultivated under biofilm and planktonic conditions. *Applied and Environment Microbiology, 71*, 2663–2676.

43. Nassar, R., Hachim, M. Y., Nassar, M., Kaklamanos, E. G., Jamal, M., Williams, D., & Senok, A. (2020). Microbial metabolic genes crucial for S. aureus biofilms: An insight from re-analysis of publicly available microarray datasets. *Frontiers in Microbiology, 11*, 3598.

44. Gries, C. M., Biddle, T., Bose, J. L., Kielian, T., & Lo, D. D. (2020). *Staphylococcus aureus* fibronectin binding protein A mediates biofilm development and infection. *Infection and Immunity, 88*, e00859–e00919.

45. Herman-Bausier, P., El-Kirat-Chatel, S., Foster, T. J., Geoghegan, J. A., & Dufrêne, Y. F. (2015). *Staphylococcus aureus* fibronectin-binding protein A mediates cell–cell adhesion through low-affinity homophilic bonds. *JAMA, 6*, e00413–e00415.

46. Menzies, B. E. (2003). The role of fibronectin binding proteins in the pathogenesis of *Staphylococcus aureus* infections. *Current Opinion in Infectious Diseases, 16*, 225–229.

47. Damo, S. M., Kehl-Fie, T. E., Sugitani, N., Holt, M. E., Rathi, S., Murphy, W. J., Zhang, Y., Betz, C., Hench, L., Fritz, G., Skaar, E. P., & Chazin, W. J. (2013). Molecular basis for manganese sequestration by calprotectin and roles in the innate immune response to invading bacterial pathogens. *Proceedings of the National academy of Sciences of the United States of America, 110*, 3841–3846.

48. Radin, J. N., Kelliher, J. L., Solórzano, P., Grim, K. P., Ramezanifard, R., Slauch, J. M., & Kehl-Fie, T. E. (2019). Metal-independent variants of phosphoglycerate mutase promote resistance to nutritional immunity and retention of glycolysis during infection. *PLoS Pathogens, 15*, e1007971.

49. Lee, H. T., Kim, S. K., Lee, J. B., & Yoon, J. W. (2019). A novel peptide nucleic acid against the cytidine monophosphate kinase of *S. aureus* inhibits staphylococcal infection *in vivo*. *Molecular Therapy - Nucleic Acids, 18*, 245–252.

50. Aravind, L., Anantharaman, V., Balaji, S., Babu, M. M., & Iyer, L. M. (2005). The many faces of the helix-turn-helix domain: Transcription regulation and beyond. *FEMS Microbiology Reviews, 29*, 231–262.

51. Pané-Farré, J., Jonas, B., Hardwick, S. W., Gronau, K., Lewis, R. J., Hecker, M., & Engelmann, S. (2009). Role of RsbU in controlling SigB activity in *Staphylococcus aureus* following alkaline stress. *Journal of Bacteriology, 191*, 2561–2573.

52. Sierra, R., Prados, J., Panasenko, O. O., Andrey, D. O., Fleuchot, B., Redder, P., Kelley, W. L., Viollier, P. H., & Renzoni, A. (2020). Insights into the global effect on *Staphylococcus aureus* growth arrest by induction of the endoribonuclease MazF toxin. *Nucleic Acids Research, 48*, 8545–8561.

53. Balemans, W., Vranckx, L., Lounis, N., Pop, O., Guillemont, J., Vergauwen, K., Mol, S., Gilissen, R., Motte, M., Lançois, D., De Bolle, M., Bonroy, K., Lill, H., Andries, K., Bald, D., & Koul, A. (2012). Novel antibiotics targeting respiratory ATP synthesis in Gram-positive pathogenic bacteria. *Antimicrobial Agents and Chemotherapy, 56*, 4131–4139.

54. Hiltunen, A. K., Savijoki, K., Nyman, T. A., Miettinen, I., Ihalainen, P., Peltonen, J., & Fallarero, A. (2019). Structural and functional dynamics of *Staphylococcus aureus* biofilms and biofilm matrix proteins on different clinical materials. *Microorganisms, 7*, 584.

55. Kulig, P., Zabel, B. A., Dubin, G., Allen, S. J., Ohyama, T., Potempa, J., Handel, T. M., Butcher, E. C., & Cichy, J. (2007). *Staphylococcus aureus*-derived staphopain B, a potent cysteine protease activator of plasma chemerin. *The Journal of Immunology, 178*, 3713–3720.

56. Sakai, Y., Kimura, S., & Suzuki, T. (2019). Dual pathways of tRNA hydroxylation ensure efficient translation by expanding decoding capability. *Nature Communications, 10*, 1–6.

57. Paranagama, N., Bonnett, S. A., Alvarez, J., Luthra, A., Stec, B., Gustafson, A., Iwata-Reuyl, D., & Swairjo, M. A. (2017). Mechanism and catalytic strategy of the prokaryotic-specific GTP cyclohydrolase-IB. *The Biochemical Journal, 474*, 1017–1039.

58. Nuxoll, A. S., Halouska, S. M., Sadykov, M. R., Hanke, M. L., Bayles, K. W., Kielian, T., Powers, R., & Fey, P. D. (2012). CcpA regulates arginine biosynthesis in *Staphylococcus aureus* through repression of proline catabolism. *PLoS Pathogens, 8*, e1003033.

59. Zhu, J. Y., Yang, Y., Han, H., Betzi, S., Olesen, S. H., Marsilio, F., & Schönbrunn, E. (2012). Functional consequence of covalent reaction of phosphoenolpyruvate with UDP-N-acetylglucosamine 1-carboxyvinyltransferase (MurA). *Journal of Biological Chemistry, 287*, 12657–12667.

60. Nakamura, A., Komatsu, M., Ohno, Y., Noguchi, N., Kondo, A., & Hatano, N. (2019). Identification of specific protein amino acid substitutions of extended-spectrum β-lactamase (ESBL)-producing *Escherichia coli* ST131: A proteomics approach using mass spectrometry. *Science and Reports, 9*, 8555.

61. Imber, M., Huyen, N. T. T., Pietrzyk-Brzezinska, A. J., Loi, V. V., Hillion, M., Bernhardt, J., Tharichen, L., Kolsek, K., Saleh, M., Hamilton, C. J., Adrian, L., Grater, F., Wahl, M. C., & Antelmann, H. (2018). Protein S-bacillithiolation functions in thiol protection and redox regulation of the glyceraldehyde-3-phosphate dehydrogenase gap in *Staphylococcus aureus* under hypochlorite stress. *Antioxidants & Redox Signaling, 28*, 410–430.

62. Chi, B. K., Gronau, K., Mader, U., Hessling, B., Becher, D., & Antelmann, H. (2011). S-bacillithiolation protects against hypochlorite stress in *Bacillus subtilis* as revealed by transcriptomics and redox proteomics. *Molecular & Cellular Proteomics*. https://doi.org/10.1074/mcp.M111.009506

63. Helmann, J. D. (2011). Bacillithiol, a new player in bacterial redox homeostasis. *Antioxidants & Redox Signaling, 15*, 123–133.

64. Loi, V. V., Harms, M., Muller, M., Huyen, N. T. T., Hamilton, C. J., Hochgrafe, F., Pane-Farre, J., & Antelmann, H. (2017). Real-Time imaging of the bacillithiol redox potential in the human pathogen *Staphylococcus aureus* using a genetically encoded bacilliredoxin-fused redox biosensor. *Antioxidants & Redox Signaling, 26*, 835–848.

65. Stancik, L. M., Stancik, D. M., Schmidt, B., Barnhart, D. M., Yoncheva, Y. N., & Slonczewski, J. L. (2002). pH-dependent expression of periplasmic proteins and amino acid catabolism in *Escherichia coli*. *Journal of Bacteriology, 184*, 4246–4258.

66. Weber, A., Kogl, S. A., & Jung, K. (2006). Time-dependent proteome alterations under osmotic stress during aerobic and anaerobic growth in *Escherichia coli*. *Journal of Bacteriology, 188*, 7165–7175.

67. Miyoshi, S. I., & Shinoda, S. (1997). Bacterial metalloprotease as the toxic factor in infection. *Journal of Toxicology Toxin Reviews, 16*, 177–194.

68. Favrot, L., Blanchard, J. S., & Vergnolle, O. (2016). Bacterial GCN5-related N-acetyltransferases: From resistance to regulation. *Biochemistry, 55*, 989–1002.

69. Luo, H. B., Knapik, A. A., Petkowski, J. J., Demas, M., Shumilin, I. A., Zheng, H., Chruszcz, M., & Minor, W. (2013). Biophysical analysis of the putative acetyltransferase SACOL2570 from methicillin-resistant *Staphylococcus aureus*. *Journal of Structural and Functional Genomics, 14*, 97–108.

70. Delgado, A., Zaman, S., Muthaiyan, A., Nagarajan, V., Elasri, M. O., Wilkinson, B. J., & Gustafson, J. E. (2008). The fusidic acid stimulon of *Staphylococcus aureus*. *Journal of Antimicrobial Chemotherapy, 62*, 1207–1214.

71. Pineda-Lucena, A., Liao, J., Wu, B., Yee, A., Cort, J. R., Kennedy, M. A., Edwards, A. M., & Arrowsmith, C. H. (2002). NMR structure of the hypothetical protein encoded by the YjbJ gene from *Escherichia coli*. *Proteins, 47*, 572–574.

72. Derewenda, U., Boczek, T., Gorres, K. L., Yu, M., Hung, L. W., Cooper, D., Joachimiak, A., Raines, R. T., & Derewenda, Z. S. (2009). Structure and function of *Bacillus subtilis* YphP, a prokaryotic disulfide isomerase with a CXC catalytic motif. *Biochemistry, 48*, 8664–8671.

73. Evans, D. A. (1989). N-acetyltransferase. *Pharmacology & Therapeutics, 42*, 157–234.

74. Tkaczuk, K. L. A., Shumilin, I., Chruszcz, M., Evdokimova, E., Savchenko, A., & Minor, W. (2013). Structural and functional insight into the universal stress protein family. *Evolutionary Applications, 6*, 434–449.

Publisher's Note Springer Nature remains neutral with regard to jurisdictional claims in published maps and institutional affiliations.